ARCHIVES OF ACOUSTICS
Vol. **44**, No. 4, pp. 793–806 (2019)
DOI: 10.24425/aoa.2019.129734

Design and Numerical Simulation of the Performance of Acoustic Plenum Chamber of a Marine Gas Turbine Air Supply System

Mehrdad RASOULIMOGHADAM, Saeid KHERADMAND*

Department of Mechanical and Aerospace Engineering
Malek-Ashtar University of Technology
P.O. Box 83145/115, Shahin-Shahr, Isfahan, Iran; e-mail: mehrdad.rasoulimoghadam@yahoo.com
*Corresponding Author e-mail: saeid_kheradmand@yahoo.com

(*received February 6, 2019; accepted July 15, 2019*)

In the present work, an approach to obtain a design method for the size of the plenum chamber cross-section of a marine gas turbine air supply system has been investigated. Flow in ducts makes noise which is very high in the turbine inlet part because of the large amount of flow. Therefore, this phenomenon should be considered in the design process. A suitable approach to design the duct is proposed (considering acoustic and aerodynamic performance at the same time). In this method, an air supply channel system of the marine gas turbine has been categorized into three sections according to the requirements of the aerodynamic and acoustic; inlet, plenum chamber, and outlet channels with circular cross-sections. The geometrical dimensions of inlet and outlet channels have been determined using the plane waves theory about a channel, in which the effects of flow is ignored. Space limitations of battleships at the dominant frequency have been considered. Then, the optimized size of the mid-channel section, in terms of both aerodynamic and acoustic requirements, using numerical methods and regarding the effects of flow has been calculated. Various 3D turbulent flows inside the plenum chamber have been considered, in which large eddy simulation turbulence model is utilized. Ffowcs, Williams and Hawkings models are used for the sound propagation process based on the Lighthill integral equation. The validity of the simulation has been checked by comparing results (sound pressure level) with experimental data obtained from a chamber. The comparison revealed the acceptable errors for a variety of frequencies. The results disclosed that the performance of channel system aerodynamic decreased when the fraction of plenum chamber cross-section to inlet/outlet channel cross-section increased. With an increase in the cross-section size at first Acoustic performance is improved and then worsen. Six different cases of marine gas turbine air supply system configurations have been presented, in which the limitation of the battleship space is considered. Examining and comparing the acoustic performance of different cases of the air supply channel system, it was found that the amount of sound pressure level, around the air supply channel system, and the high-pressure sound area can move along the air supply channel system. Additionally, deviations from plane waves considering the effects of flow have been inspected in all cases. The reason for this deviation is the effects of the airflow through the channel system and quadrupole sources in the production of sound in the channel system, which causes higher modes.

Keywords: aeroacoustics; large eddy simulation; Lighthill analysis; Ffowcs Williams model; Hawkings model; propagation of wave in duct.

1. Introduction

Battleships need large power to reach the speed and power of maneuver. If the power is only provided by the diesel engine, the diesel engine must be very large and extremely noisy. One of the most effective ways to increase the maneuverability of a battleship is to use the gas turbine to produce the required propulsion power. On the other hand, if the propulsion power is provided in all battleship states (maneuverable and non-maneuvering) using a gas turbine, the consumption of battleship fuel will increase significantly (gas turbine consumes a lot of fuel). Therefore, to solve those problems, the combination of a diesel engine and the gas turbine is suggested. In this combination, the required propulsion power is provided by a diesel engine, when the battleship is not in maneuvering state and moves at an average speed. Besides, when it is on

maneuvering state for a limited time, it is supplied by a gas turbine. Thus, to have a high maneuvering battleship, which is good for both fuel consumption and the size of the engine room, a combination of the diesel engine and gas turbine seems an acceptable approach. Considering the fact that the gas turbine is located in a closed environment (engine room), the main objectives should be provided with the required air. The gas turbine absorbs the required air by the suction of its compressor through the air supply system from the outside of the engine room (free space). The important challenge here is to produce very high noise in the air supply system. That is because of the operation of the gas turbine and the severe airflow, which is caused by a high mass flow rate generated by the gas turbine. Since the engine room is located at the bottom of the battleship floor (underwater), the generated noise damages battleship crews and enters the battleship space through the water. It is very vital because it may help enemy submarine radar to detect the battleship. Therefore, the purpose of the present work is to study the noise generated around the marine gas turbine air supply system and how it can be reduced. The schematic representation of the marine gas turbine air supply system is shown in Fig. 1.

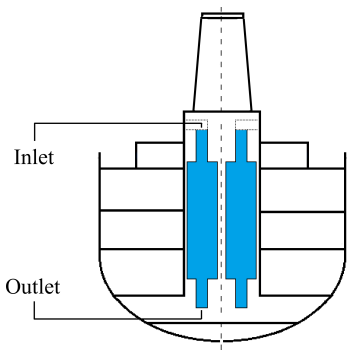

Fig. 1. Two-dimensional schematic view of the marine gas turbine air supply system from the battleship deck to the marine gas turbine compressor.

In general, the noise coming from the fluid flow is generated by the formation of vortices, and the presence of friction along the channel wall, which can also have an important role in the process of transfer and distribution of the fluid. Studies show that, by a reduction in the diameter of the channel inlet, the level of sound intensity along the length of the channel continuously increases (Cao *et al.*, 2017; Liu *et al.*, 2016; Mak *et al.*, 2014; Nag *et al.*, 2017). In order to simulate and predict the noise generated by the flow in the sound reduction system, the first step is to simplify the general system model and to determine the main sources of sound generated within the fluid flow (Guasch *et al.*, 2017; Hillenbrand *et al.*, 2016; Maizi *et al.*, 2018; Warczek *et al.*, 2017). After simplifying the system, it is important to determine the proper method to predict the flow noise caused by the nature of the flow. In this area, methods for subsonic flows and small-scale systems were presented in (Alkan, Atayilmaz, 2018; Guasch, 2016; Nag *et al.*, 2017; Peng *et al.*, 2018). In order to study the acoustic performance of systems on a large scale, the traditional method constituting Finite Element Method (FEM), Boundary Element Method (BEM), the four-polar matrix method and the three-point method have been used. The best way of studying the acoustic performance of these systems is the FEM method. The three-point method is also the fastest method and is easy to use; whereas, the quadruple method is not so straightforward to deal with (Bilawchuk, Fyfe, 2003; Dube *et al.*, 2018). The acoustic performance of the expansion chamber depends on the cross-sectional area; so that, the transmission loss parameter decreases if the diameter of the expansion chamber increases (Cao *et al.*, 2017; Łapka, 2014; Nag *et al.*, 2017; Zhang *et al.*, 2009). In the low-frequency range, the transmission loss values are equal to the results obtained from the plane wave theory. Whereas, in higher frequency ranges, the reduction in transferred quantity are exponentially converted to those obtained from the plane wave theory; the observed errors come from the propagation of sound waves in higher modes at higher frequencies (Chiu, Chang, 2014; Wu *et al.*, 2007; 2008). In addition, the intensity of plane waves reflection at low frequencies, in which physical barriers exist, is higher than that of high frequencies. This intensity reduces the propagation of plane waves from noise sources because of destructive interference of the plane waves at low frequencies (Kĺrekull *et al.*, 2014). In a small expansion chamber, the resonance phenomenon occurs unexpectedly at lower frequencies than the cut-off frequency. Therefore, to eliminate unstable modes, the length of the expansion chamber must be very small (Ji, 2005). Totally, the theory of plane waves is not acceptable for the length of an equivalent knee housing (Chu *et al.*, 2001; Vizzini *et al.*, 2018). In backflow muffler, if the expansion chamber length is half of the wavelength, the transfer reduction curve decreases to its lowest value. Also, the highest transfer loss, even if the length of the muffler does not increase, can occur at low frequencies (Mohammed *et al.*, 2012). The most important parameter affecting the acoustic performance of the resonator (perforated tube) is porosity in the absence of flow-free effects. Besides, for short or long resonators, by increasing porosity, the frequency at which the main noise reduction occurrence increases. Considering fluid flow's effects, it is noticed that more parameters will be effective in the acoustic performance of the resonators. In short resonators, as porosity rise, the frequency and amplitude of the noise reduction parameter increase; in contrast, in long resonators, acoustic performance decreases into a range

of desired frequencies. The average flow velocity also has a significant effect on the acoustic performance of the resonator. In short resonators, the more average flow rate rises, the more reduction in transmission loss parameter occurs (Tsuji *et al.*, 2002).

Researches indicate that, so far, there have been no specific efforts on an investigation of the performance of large-scale plenum chamber and special applications (such as the gas turbine plenum chamber with a high intake air flow rate) introducing any specific design process. The design process presented in this paper seems to be a good tool to design these products from two perspectives: the pressure loss in a plenum chamber and the amount of sound produced by the flow of air from the plenum chamber. On the other hand, in order to conduct an aeroacoustic analysis about various issues, the fluid flow field from two aspects needs to be examined thoroughly: numerical solution of the fluid flow field (Computational Fluid Dynamics) and numerical solution of the acoustic field. The calculation costs of these studies using the available software packages, especially for these specific applications, would be massive. In the present work, attempts have been performed to reduce the computational cost by changing and introducing an alternative tool for the numerical solution of an acoustic field.

2. Governing equations and introduction of parameters

2.1. Acoustic elements of the marine gas turbine air supply system

After examination of all types of elements used in sound reduction systems in the marine gas turbine air supply system, two different elements have been chosen considering the available space in battleships:

(a) First-type element

This element is the equivalent of a channel with a uniform cross-section (Fig. 2a). Assuming that only the plane waves can be propagated in this type of element, the specific acoustic impedance at each point of the standing wave field is defined as (Munjal, 1987):

$$\xi(z) = \frac{p(z)}{v(z)} = Y_o \frac{Ae^{-jk_o z} + Be^{jk_o z}}{Ae^{-jk_o z} - Be^{jk_o z}}, \tag{1}$$

where ξ, p, v, and Y_o are specific acoustic impedance, acoustic pressure, mass velocity, and acoustic impedance of the channel, respectively. A and B are exponential terms related to time and k_o is the wave number, which is calculated by (Munjal, 1987):

$$k_o = \frac{\omega}{a_o} = \frac{2\pi}{\lambda}, \tag{2}$$

where a_o, ω, and λ represent the velocity of sound emission in the wave propagation environment, angular velocity, and wavelength, respectively. According

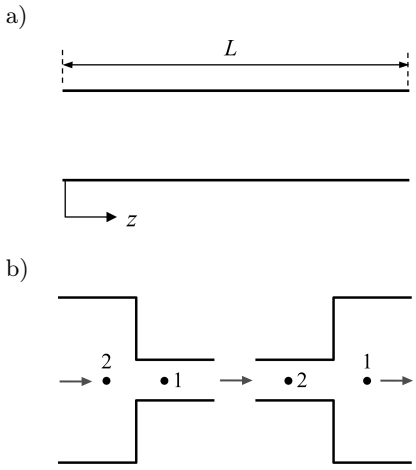

Fig. 2. Schematic representation of acoustic elements: a) first-type acoustic element, b) second-type acoustic element.

to Fig. 2a, for the specific acoustic impedance at the first and last section of the channel, we have (Munjal, 1987):

$$\xi(0) = Y_o \frac{A+B}{A-B}, \tag{3}$$

$$\xi(L) = Y_o \frac{Ae^{-jk_o L} + Be^{jk_o L}}{Ae^{-jk_o L} - Be^{jk_o L}}. \tag{4}$$

In Eq. (4), L is the length of the channel. Considering the equations, we can write (Munjal, 1987):

$$\xi(0) = \frac{\xi(L)\cos(k_o L) + jY_o \sin(k_o L)}{j\left(\frac{\xi(L)}{Y_o}\right)\sin(k_o L) + \cos(k_o L)}. \tag{5}$$

At low frequencies or the case of very small channels $\left(k_o^2 L^2 \ll 1\right)$, it can be written:

$$\cos(k_o L) \cong 1, \qquad \sin(k_o L) \cong k_o L. \tag{6}$$

So Eq. (5) can be rewritten as follows (Munjal, 1987):

$$\xi(0) = \frac{\xi(L) + jY_o k_o L}{j\left(\frac{\xi(L) k_o L}{Y_o}\right) + 1}, \tag{7}$$

$$\xi(0) = \frac{\xi(L) + \frac{j\omega L}{S}}{j\left(\frac{\xi(L)\omega V}{a_o^2}\right) + 1} = \frac{\xi(L) + Z_M}{j\left(\frac{\xi(L)}{Z_C}\right) + 1}. \tag{8}$$

In Eq. (8), S is the cross-sectional area of the channel, V represents channel volume, Z_M shows the total impedance of the channel, and $1/Z_C$ is the total admittance of the channel. If $\xi(L) \ll Z_c$, then Eq. (5) can be written as follows (Munjal, 1987):

$$\xi(0) \cong \xi(L) + Z_M. \tag{9}$$

The channel is connected to a larger one having a larger cross-section. The resistance Z_M is closed

in a circuit at lumped-element representation (Fig. 3a). If $Z_M \ll \xi(L)$, then Eq. (5) can be written as follows (Munjal, 1987):

$$\xi(0) \cong \frac{\xi(L) Z_C}{\xi(L) + Z_C}. \tag{10}$$

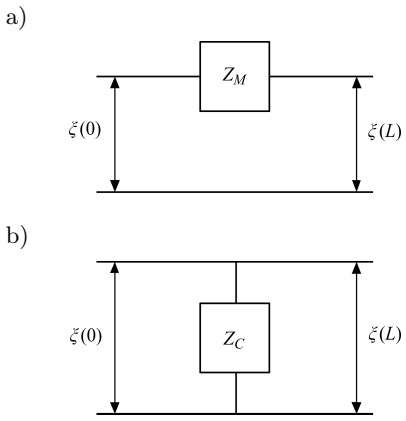

Fig. 3. Lumped-element representation of a channel: a) the channel as a lumped in-line inertance, b) the channel as a shunt compliance.

This time, the channel is connected to a small one with a smaller cross-section. The resistance Z_c is closed in parallel at lumped-element representation (Fig. 3b) (Munjal, 1987).

(b) Second-type element

The second-type element is equal to the case of a sudden change in the cross-section of the channel (Fig. 2b). If the dimensions of both cross-sections are chosen so that plane waves can propagate in them, then, the acoustical pressure and mass velocity are equal in both cross-sections (Munjal, 1987):

$$p_2 = p_1, \tag{11}$$

$$v_2 = v_1. \tag{12}$$

Therefore:

$$\xi_2 = \frac{p_2}{v_2} = \frac{p_1}{v_1} = \xi_1. \tag{13}$$

Due to the constant values of ξ, v and p, this type of element cannot be shown in a lumped-element circuit. However, in acoustic terms, these are sudden changes in the middle section of the low pass filters.

2.2. Geometrically determination of the marine gas turbine air supply system

Three elements of the first-type ($n = 3$), which include a, b, and c, have been chosen for the marine gas turbine air supply system (expansion chamber/muffler). These elements were connected by second-type elements (points 1 and 2). Two-dimensional schematic representation of the marine gas turbine air supply system and its equivalent lumped-element are shown in Fig. 4.

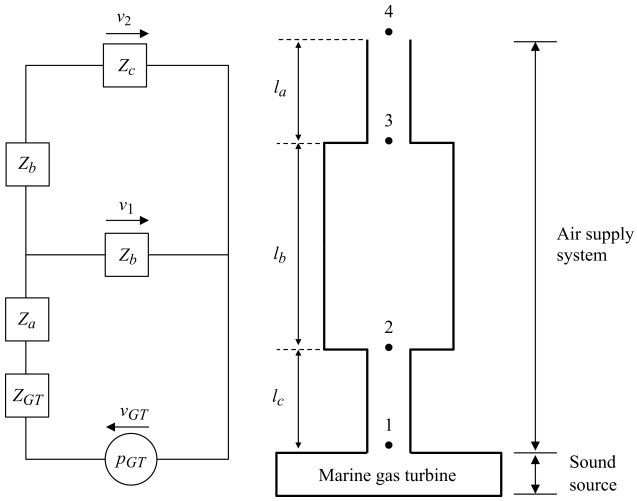

Fig. 4. Schematic representation of the system and its lumped-element representation.

2.3. Aerodynamic equations

In the aerodynamic analysis of the flow of the channel system, two equations of continuity and momentum govern the fluid motion. These equations are defined in Eqs (14) and (15), in which ρ, u_i, P, and υ are fluid density, components of fluid flow velocity, pressure, and kinematic fluid viscosities, respectively (Munjal, 1987):

$$\frac{\partial \rho}{\partial t} + \frac{\partial}{\partial x_i}(\rho u_i) = 0, \tag{14}$$

$$\frac{\partial u_i}{\partial t} + u_j \frac{\partial u_i}{\partial x_i} = -\frac{1}{\rho}\frac{\partial P}{\partial x_i} + \upsilon \frac{\partial^2 u_i}{\partial x_i \partial x_j}. \tag{15}$$

2.3.1. Navier-Stokes equations filtered in incompressible state

Applying changes into Navier-Stokes equations and separating large and small vortices, the final equations (large-eddy equations) are presented as follows (Pierre, 2001; Wilcox, 1998):

- Continuity equation:

$$\frac{\partial \overline{u}_i}{\partial x_i} = 0, \tag{16}$$

- Momentum equation:

$$\frac{\partial \overline{u}_i}{\partial t} + \frac{\partial}{\partial x_i}\left(\overline{u_i u_j}\right) = -\frac{1}{\rho}\frac{\partial \overline{p}}{\partial x_i} + \upsilon \frac{\partial^2 \overline{u}_i}{\partial x_j x_j} + \frac{\partial \tau_{ij}}{\partial x_j}, \tag{17}$$

τ_{ij} represents the properties of tiny vortices which are defined as follow:

$$\tau_{ij} = \overline{u_i u_j} - \overline{u}_i \overline{u}_j. \tag{18}$$

2.3.2. Smagorinsky turbulence model

In the Smagorinsky turbulence model, according to Boussinesq approximation, the non-isotropic part of stress τ_{ij} is associated with a large turbulent viscosity (S_{ij}) based on the Eq. (19). The remainder of the stress and isotropic part $\frac{1}{3}\tau_{kk}$ is put into the pressure (Pierre, 2001; Wilcox, 1998):

$$\tau_{ij} - \frac{1}{3}\tau_{kk}\delta_{ij} = -2\upsilon_t \overline{S}_{ij}. \tag{19}$$

The deformation tensor is defined in terms of the velocity of the large vortices (Pierre, 2001; Wilcox, 1998):

$$\overline{S}_{ij} = \frac{1}{2}\left(\frac{\partial \overline{u}_i}{\partial x_j} + \frac{\partial \overline{u}_j}{\partial x_i}\right). \tag{20}$$

Also, the eddy viscosity is defined in terms of length:

$$\upsilon_t = l^2 \left|\overline{S}\right|, \tag{21}$$

where

$$\left|\overline{S}\right| = \sqrt{2\overline{S}_{ij}\overline{S}_{ij}}, \tag{22}$$

l is the longitudinal scale of the tiny vortices defined as a coefficient of the network dimension Δ (Pierre, 2001; Wilcox, 1998):

$$l = C_s \Delta. \tag{23}$$

In which, C_s (Smagorinsky's constant) controls the amount of turbulence and depends on the type of flow. This coefficient is usually applied between 0.065 and 0.25 and its theoretical value is calculated to be 0.16 (Pierre, 2001).

2.4. Noise generation resources

The general relationship between the production and propagation of acoustic waves is (Howe, 2003; Wang *et al.*, 2006)

$$\frac{1}{a_0^2}\frac{\partial^2 p'}{\partial t^2} - \nabla^2 p' = q, \tag{24}$$

q is equal to the sources of noise and p' represents fluctuations in the pressure of the fluid flow, which is defined as $p' = p - p_0$ (p_0 is the pressure in the equilibrium state of the fluid). The three main sources of noise generation are mass production, momentum change, and nonlinear sources (such as turbulent flow). Other sources, such as chemical and thermal reactions can be origins of serious noise generation (Howe, 2003; Wang *et al.*, 2006).

2.5. Lighthill analysis

The nonhomogeneous Lighthill wave equation is defined for density fluctuations (Howe, 2003; Wang *et al.*, 2006):

$$\frac{\partial^2 \rho'}{\partial t^2} - a_0^2 \frac{\partial^2 \rho'}{\partial x_i^2} = \frac{\partial^2 T_{ij}}{\partial x_i \partial x_j}, \tag{25}$$

ρ' is the density fluctuation defined as $\rho' = \rho - \rho_0$ (ρ_0 is the density in the equilibrium state of the fluid), and T_{ij} is the Lighthill stress tensor which can be obtained by (Howe, 2003; Wang *et al.*, 2006):

$$T_{ij} = \rho u_i u_j + \delta_{ij}\left(p' - a_0^2 \rho'\right) - \sigma_{ij}. \tag{26}$$

It is assumed that there are some limitations to noise sources which are in a steady form of the fluid and have a sound speed of a_o. In such an environment, waves are propagation as isentropic and those waves can be heard by listeners, can be expressed inside the fluid at a point x and at a time t (Dawkins, 2011; Howe, 2003; Lighthill, 1952; Norton, Karczub, 2003; Wang *et al.*, 2006)

$$\frac{1}{a_0^2}\frac{\partial^2 p'}{\partial t^2} - \frac{\partial^2 p'}{\partial x_i \partial x_j} = \frac{\partial \dot{Q}}{\partial t} - \frac{\partial F_i}{\partial x_i} - \frac{\partial^2 T_{ij}}{\partial x_i \partial x_j}. \tag{27}$$

The first part of the equation is a monopole source that is commonly used in rotary machines and also called noise thickness. This term indicates fluid displacement by blades of a rotary machine and shows that if the mass flow rate changes in an unsteady state, noise is produced. If the velocity of the blades is low or blades themselves are thin, then monopole sources have little contribution to noise generation. The second part of Eq. (27) is a dipole source showing that if at different times forces are applied to the fluid, noise is generated. For fixed surfaces (such as a channel), these unstable surface loads lead to the production of fixed dipole sources and at the rotational surfaces (such as the rotation of a fan in the fluid flow), it generates a rotating dipole source. In both cases, when the flow is inherently subsonic, it is expected that the dominant sources in the production of sound are dipole sources. The third term of Eq. (27) represents the quadrupole source which is related to nonlinear effects (time-dependent stresses, momentum, viscosity, and turbulence). In fact, the turbulent flow can be a source of it. For subsonic rotary machines, the effect of the quadrupole source is neglected. It is important to consider that the existence of fluid mass with constant density is not a source of the noise. Also, the constant of the force applied to the fluid does not produce any noise (Howe, 2003; Wang *et al.*, 2006).

2.5.1. Lighthill integral equation

The original method proposed by Lighthill to solve the nonhomogeneous wave equation leads to an integral formulation. This method is based on the use of

the free space green function in the infinite domain. Using this method, the final formula for solving Eq. (28) is as follows:

$$\rho'(x,t) = \frac{1}{4\pi a_0^2}\frac{\partial^2}{\partial x_i \partial x_j}\int\limits_{\Omega}\frac{T_{ij}\left(y, t-\frac{|x-y|}{a_0}\right)}{|x-y|}\,\mathrm{d}y. \quad (28)$$

In Eq. (28), x is noise receiver position vector, y is noise source position vector, a_0 is the speed of sound and Ω is the domain of integration on the volume in which the turbulence generates noise. This domain should cover all sources of noise. Solving Eq. (28), the density fluctuations are obtained for the receiver of noise at position x at time t.

2.5.2. Ffowcs Williams and Hawkings model

In the Lighthill integral equation, it is assumed that there is no solid plate in the fluid flow and even if it exists, its effect is ignored. Hence, Ffowcs Williams and Hawkings developed the Lighthill formula in the form of solid plates in the fluid flow, known as formula FW-H in aero-acoustics and are given in Eq. (29) (Howe, 2003; Wang *et al.*, 2006)

$$\frac{\partial^2\rho'}{\partial t^2} - a_0^2\frac{\partial^2\rho'}{\partial x_i^2} = \frac{\partial^2\overline{T}_{ij}}{\partial x_i\partial x_j} - \frac{\partial}{\partial x_i}\left(P_{ij}\delta(f)\frac{\partial f}{\partial x_i}\right) + \frac{\partial}{\partial t}\left(\rho_0 v_i\delta(f)\frac{\partial f}{\partial x_i}\right). \quad (29)$$

The integral expression of the FW-H equation for the density fluctuations is as follows:

$$\rho'(x,t) = \frac{1}{4\pi a_0^2}\frac{\partial^2}{\partial x_i\partial x_j}\int\limits_{\Omega}\frac{T_{ij}\left(y, t-\frac{|x-y|}{a_0}\right)}{|x-y|}\,\mathrm{d}y - \frac{1}{4\pi a_0^2}\frac{\partial^2}{\partial x_i\partial x_j}\int\limits_{\Omega}\frac{P_{ij}n_j\left(y, t-\frac{|x-y|}{a_0}\right)}{|x-y|}\,\mathrm{d}y + \frac{1}{4\pi a_0^2}\frac{\partial^2}{\partial t^2}\int\limits_{\Omega}\frac{\rho_0 v_n}{|x-y|}\,\mathrm{d}y. \quad (30)$$

In addition to flow turbulence, this integral equation considered the pressure fluctuations and the effects of the motion of rigid plates in the flow as sources of noise (Howe, 2003; Wang *et al.*, 2006).

2.6. Sound pressure level

Sound Pressure Level (SPL) is a logarithmic measure of the effective pressure of a sound relative to a reference value that measured as dB and defined by:

$$\mathrm{SPL} = 20\log_{10}\left(\frac{p}{p_0}\right), \quad (31)$$

p is the root mean square sound pressure and p_0 is the reference sound pressure which is often considered as the threshold of human hearing (Bies *et al.*, 2017).

3. Simulation

3.1. Modeling and boundary conditions

The marine gas turbine air supply system is simulated according to the aerodynamic and acoustic requirements. It is performed for the different fraction of inlet (or outlet) area to plenum chamber area and also for the different position of the inlet and outlet element relative to the position of the plenum chamber. The task of an air supply system is to transfer air from the surrounding area to the desired space. In order to carry out this task, the system design must be defined within the framework of available facilities and instructions that are defined for the limits of the pressure drop, airflow speed, sound level, etc. The required airflow rate for a specific marine gas turbine is 66 kg/s. Due to the suction of gas turbine compressors, this amount of air from the atmospheric around the battleship reaches the gas turbine engine through the air supply system. Therefore, the inlet boundary condition is defined as a mass flow inlet. Since information about the flow conditions in the air supply system outlet is rare, the outflow boundary condition is chosen as the outlet flow condition. For the walls of the channel, the boundary condition of the wall is adapted.

3.2. Numerical method

In this simulation, a hybrid approach has been used. At the first step before acoustic calculations, the flow transient numerical solution must be implemented using computational fluids dynamical software which has reached a stable state (that is, the convergence is solved). This means that the unsteady flow under considerations including all the main variables of the stream fully developed and does not change over time. Methods of Reynolds Average Navier-Stokes equations, Direct Navier-Stokes equation, and Large Eddy Simulation are all options for the solution of flow transitions. In this simulation, in order to evaluate the aerodynamic performance of the system (the study of the production of sound sources in the system), the Large Eddy Simulation method ($y^+ < 1$) and an open-source software have been used. A conventional method to obtain flow transitions is to use the steady-state solution as the initial guess. To solve the steady state and aerodynamic analysis of the air supply system, considering the geometry of the cross-sectional channel, the $k-\varepsilon$ turbulence model has been used. Also, in order to evaluate the acoustic performance of the system (sound propagation in the environment), Lighthill's analogy and, FW-H method and an open-source software have been used.

3.3. Validation

To validate the process of simulation the marine gas turbine air supply system, the results have been compared with the outcomes from an experimental study on an expansion chamber having the circular cross-section. Munjal *et al.* (1997) studied empirically the acoustic performance of an expansion chamber with an inlet and an outlet flowing through a stream of the Mach number 0.1. The schematic view of the expansion chamber is shown in Fig. 5, in which $L = 0.3$ m, $l_a = 0.15$ m, $\frac{R}{r} = 5$, $R = 0.061$ m.

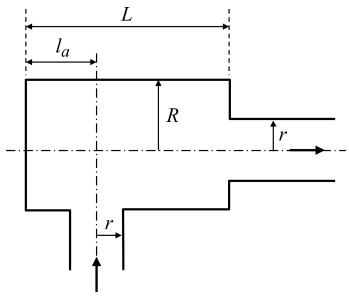

Fig. 5. Schematic view of the model by (Munjal, 1997).

The results obtained from this simulation is depicted in Fig. 6.

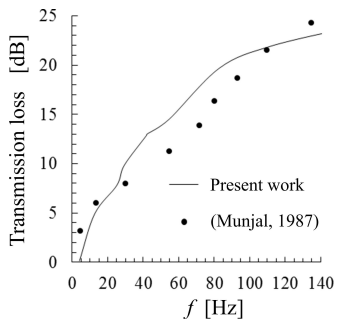

Fig. 6. Comparison of the transmission losses of expansion chamber that obtained from numerical solution with experimental data.

The graph of the SPL absolute error of the numerical results is compared to the experimental data (Fig. 7).

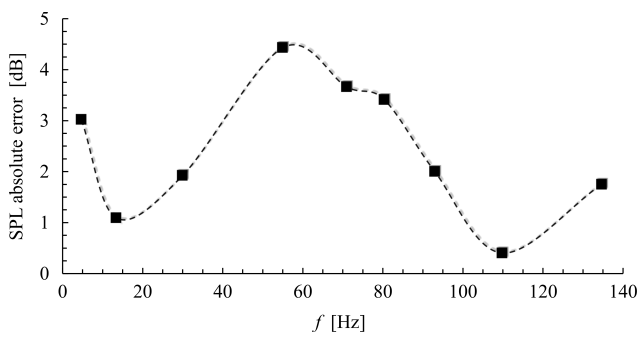

Fig. 7. SPL absolute error of the numerical results compared to experimental data at various frequencies.

As it is seen, the highest numerical error compared to the experimental data at low frequencies is 4.5 dB, which occurred at a frequency of 55 Hz. It seems that the accuracy of the entire frequency range studied in this area depends on the type of flow (turbulent flow), random nature and turbulent flow models. On the other hand, the frequency range studied has been chosen according to its importance in marine applications (underwater).

4. Results

4.1. Marine gas turbine air supply system design method

In order to design the marine gas turbine air supply system, the following steps should be performed:

- Determination of the length of the acoustic components of the air supply system, without considering the effects of flow, in order to prevent the resonance phenomenon and according to the length of the whole air supply system.
- Determination of the geometric shape and cross-sectional dimension of the acoustic elements (inlet and outlet) of the system considering the effects of airflow and according to the marine standards, the Mach number flow through the system and its pressure drop.
- Determination of the appropriate cross-sectional dimension the most important acoustic element (plenum chamber element), taking into account the effects of airflow and according to the aerodynamic and acoustic requirements of the air supply system.
- Examination of the acoustic performance of the air supply system without considering the flow effects (marine gas turbine starter conditions) and with regard to the effects of flow passage (full load marine gas turbine condition).
- Examination of the acoustic performance of the marine gas turbine air supply system in different cases of the inlet and outlet element relative to the position of the plenum chamber with considering the effects of flow (full load marine gas turbine condition).

4.2. Geometric characteristics of the marine gas turbine air supply system, without considering the effects of flow

Schematic representation of the length of the elements of the marine gas turbine air supply system is shown in Fig. 8. A frequency of sound waves that can be propagated in the air supply system depends on the frequency of the source of them; that is, the airflow through the air supply system by the suction of

the marine gas turbine compressor. Because of different engine RPMs, operating conditions of the marine gas turbine, the average frequency of the sound waves propagated in the air supply system (the dominant frequency), in steady-state and full load is 23 Hz. The length of the expansion chamber elements (air supply system) has a great influence on their acoustic performance. As a general criterion in design, when the element length is odd multiples of one-fourth of the wavelength of the sound, the occurrence of a resonance phenomenon is prevented and most acoustical damping is performed by the element (Ji, 2005).

$$l_e = \frac{n\lambda}{4} = \frac{na_o}{4f}, \qquad n = 1, 3, 5, \ldots \tag{32}$$

Due to the average amount of frequency produced in the air supply system, the appropriate length for each of the elements is:

$$l_e = \left(\frac{346}{4 \cdot 23}\right) n \cong 4n, \qquad n = 1, 3, 5, \ldots \tag{33}$$

Considering the equation and taking into account the fact that the most important element of the marine gas turbine air supply system is the element b, the length of it should be taken odd multiples from 4 m. On the other hand, according to the battleship structure, the maximum length of the air supply system is about 8 m. So, the length of the element b is chosen as 4 m. In this case, the length of the other two elements assuming they have the same lengths, it will be 2 m. The size of the cross-section and the speed of sound propagation in air supply system are the parameters that influence the frequency and how the sound waves propagate through the system at higher mods. In other words, if the frequency is small enough, only the plane sound waves can be propagated in the air supply system (Munjal, 1987):

$$f < \frac{\pi a_o}{1.84D}(1 - M^2)^{0.5}. \tag{34}$$

According to marine standards and aerodynamic criteria, the cross-section of the expansion chamber elements is chosen as a circular one. Besides, increasing the speed of airflow through the air supply system, the more noise will be generated. The amount of pressure drop in the turbulent flow is proportional to U^n, in which $1.8 \leq n \leq 2$ (Nakayama, Boucher, 1998). Therefore, according to the above criteria and the amount of space available in the battleship aiming for reduction of the Mach number of air supply system flow ($M < 0.3$), the radius of the cross-section (elements a and c) was chosen as 1 m.

4.3. Determination of the cross-sectional dimension of the plenum chamber of the marine gas turbine air supply system, with considering the effects of flow

A sudden change in the cross-section of the air supply system in aerodynamics causes a sharp drop in the pressure of the fluid flow and in acoustics. Also, it improves and increases the damping property of the air supply system. In this stage of design, using the simulation process the most appropriate ratio of area $m = S_b/S_a$ is determined, which has the highest acoustic performance and aerodynamically the least amount of pressure drop in airflow. The numerical solution for the five area ratio values was performed. In each case, in addition to the determination of an amount of pressure drop in the air supply system, the sound pressure level at the test point, located 6 meters from the channel axis and at a distance of 4 meters from the channel entrance, was calculated (Fig. 8).

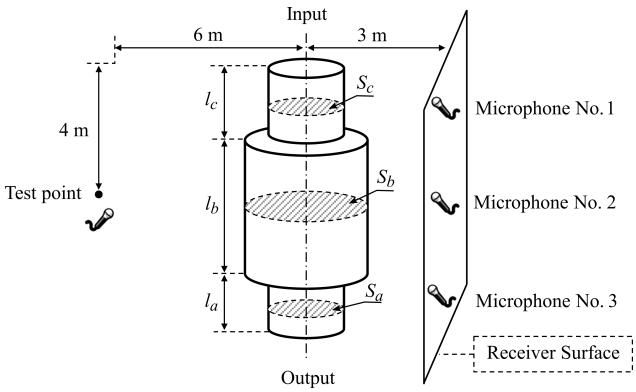

Fig. 8. The location of the test point in the study of the cross-sectional area of the plenum chamber of the marine gas turbine air supply system, and location of noise receivers around it (receiver surface).

The system pressure drop and the sound pressure level at the test point for various values of the parameter m are shown in Fig. 9.

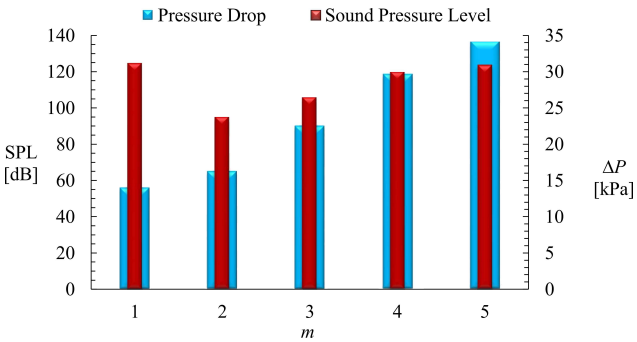

Fig. 9. The pressure drop of the marine gas turbine air supply system and the sound pressure level at the test point for different values of the area ratio.

As it is observed, by increasing area ratio, the pressure drop of the air supply system goes up and the sound pressure level at the test point initially reduces and then rises. Rising in area ratio, the vortex power and the intensity of the separation of flow in the sudden change in the cross-sectional area experienced the substantial rise and also, the wider range of fluid flow field is affected. As a result, pressure fluctuates

inside the air supply system increases. Furthermore, in a sudden reduction of the cross-section, dead areas will grow with larger vortices and high turbulence and will absorb more energy from the airflow reducing the ability to work (total pressure). In small values of the ratio of the areas ($1 < m < 3$), the vortexes size in the element b are smaller than that of the system without this element; thus, it produces less noise. Since this propagation of the waves is instantaneous and random, due to the destructive interference of these waves, a fraction of their power is neutralized. Increasing the area ratio ($m \geq 3$), the size and strength of the vortices in the element b increase. As a result, flow turbulence and sound waves produce greater power. In the design of ducts, especially those for gas turbines, the maximum allowable pressure drop of the air supply duct is estimated at approximately 15 kPa. In these circumstances, the reduction in pressure does not have a significant effect on the operation of the gas turbine. Therefore, based on these items and severe restrictions on the space of battleships, the expansion area ratio of 2 has been selected. As a result, the cross-section of element b is 6.28 m^2, and its diameter, 2.83 m. Due to the cross-sectional dimension of element b, the average Mach number of this element is 0.025 and the mode frequency (0, 0) is 208.7 Hz, which is much larger than the dominant frequency of the system. Therefore, it can be said that in this element, irrespective of the effects of the flow passage, only plane waves can be propagated.

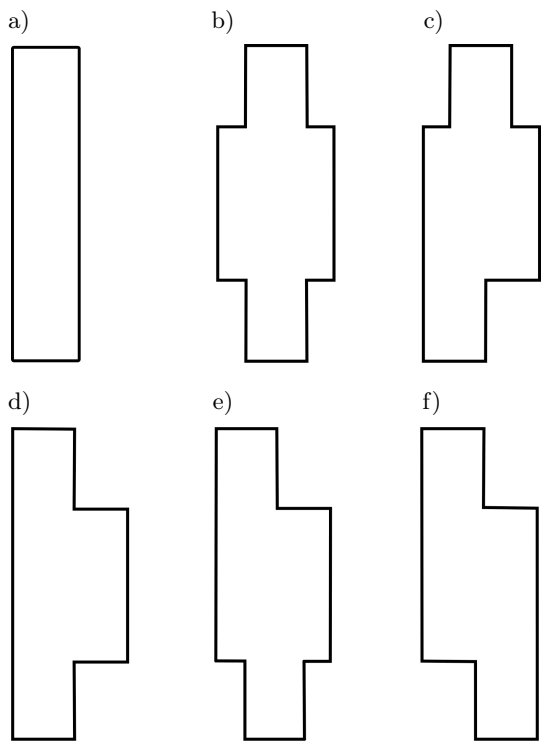

Fig. 10. Schematic representation of different cases of evaluation of the acoustic performance of the marine gas turbine air supply system; a) case 1: without plenum chamber, b) case 2: end inlet/end outlet/on center, c) case 3: end inlet-on center/end outlet-side, d) case 4: end inlet/end outlet/side, e) case 5: end inlet-side/end outlet-on center, f) case 6: end inlet/end outlet/offset.

4.4. Acoustic performance evaluation of the marine gas turbine air supply system

The acoustic performance of marine gas turbine air supply systems in different cases of inlet and outlet element relative to the position of the plenum chamber in low pass filter (LPF) and in the range of 1 Hz to 100 Hz (bandwidth) has been studied. The schematic view of the different configurations of the air supply system is shown in Fig. 10.

Marine environments are usually quieter and more stable than the real environment of human being lives. Also, they have a high dampening effect and high noise absorption. So, the highest emission distance of sounds produced and propagated at high frequencies in the marine environments is very small in comparison with the case of low frequencies. For that, submarines use low frequencies for communication, identification, and etc. which are called "Sonar Frequency" (Carlton, 2012). Thus, the frequency range is limited to the sonar frequencies between 1 to 100 Hz which are militarily important in the marine environment and can be detected by submarine radars. In this step, the acoustic performance of the marine gas turbine air supply system in the frequency range of 1 to 100 Hz has been examined. It is done particularly at the frequency of 23 Hz, in order to study the propagation of plane waves in it.

According to the geometric shape of the air supply system, the geometric locations of the receivers (the position of the microphones) have been considered on a page with a length 8 m (total length of the air supply system) and a width of 4 m, located 3 m from its symmetry axis. Also, to determine the acoustic performance of each air supply system elements in other frequencies, microphones 1, 2, and 3 located in the middle of the length of each element and on the receiver surface (Fig. 8).

4.4.1. Acoustic performance evaluation of the marine gas turbine air supply system in the sonar frequency range

In Figs 11, 12, and 13, the sound pressure level graph in the microphones 1, 2, and 3 are shown in different air supply system cases.

The average of different levels of a sound pressure level in an environment was calculated as follows:

$$\overline{\mathrm{SPL}} = 10\log\left(\frac{1}{n}\sum_{i=1}^{n} 10^{\frac{\mathrm{SPL}_i}{10}}\right). \tag{35}$$

According to Figs 11, 12, and 13, the average sound pressure level in microphones 1, 2, and 3, in different

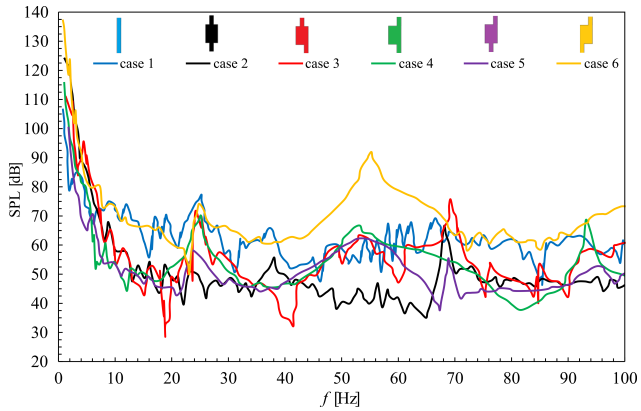

Fig. 11. Sound pressure level around the inlet of the marine gas turbine air supply system (microphone No. 1).

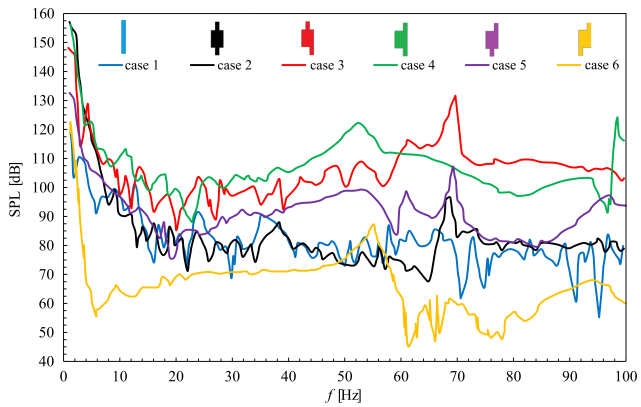

Fig. 12. Sound pressure level around the plenum chamber of the marine gas turbine air supply system (microphone No. 2).

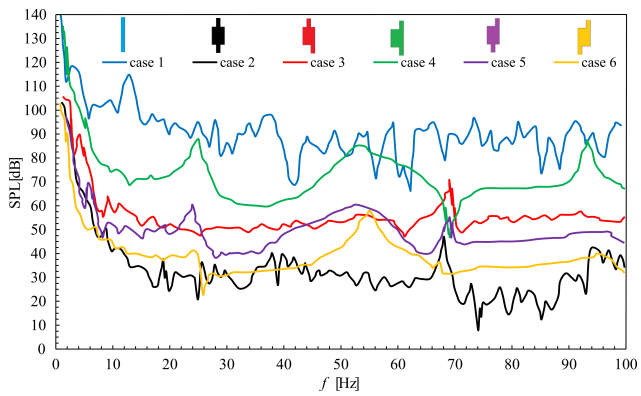

Fig. 13. Sound pressure level around the outlet of the marine gas turbine air supply system (microphone No. 3).

cases of the inlet and outlet element relative to the position of the plenum chamber is shown in Fig. 14.

In case 1, the average sound pressure level increases with flow progression along the air supply system axis. This is because the channel path is completely continuous and uniform, and there is no sudden change in the cross-section as well as in its path. As a result, the boundary layer will grow continuously. Besides, the

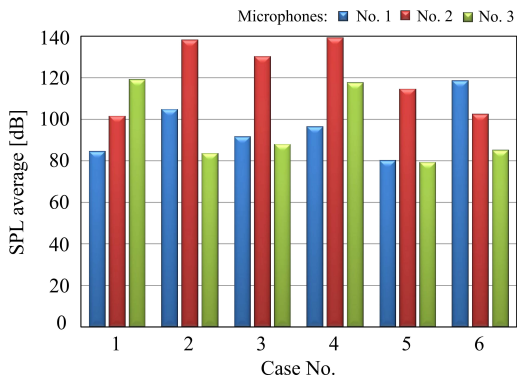

Fig. 14. The average sound pressure level in different cases of input and outlet element relative to the position of the plenum chamber.

size and strength of the vortices flow increases and increases the sound pressure level.

In case 2, the average sound pressure level is increased by moving the flow along the air supply system axis, and then decreases less than its value at the channel entrance. This is due to the fact that with the progression of the flow inside the air supply system, the sudden change in the cross-section of the channel air supply system, the boundary layer and the permeation vortices in the fluid flow are not allowed to grow. However, the average sound pressure level at the channel inlet (microphone 1) is 20 dB more than in case 1. As flow into the plenum chamber, the average flow velocity reduces and in the corners of the plenum chamber, weak vortices are produced. These vortices cause that areas in the middle of the channel (microphone 2) have the average sound pressure level of 36 dB more than case 1. As the flow reaches the end in the channel, the average velocity of the flow increases and the sharp edges cause the flow separation in this section. Given the geometric shape of the image, the strength of this separation is small and it causes the size of larger vortices to be attenuated. As a result, the average sound pressure level at the channel outlet (microphone 3) drops about 35 dB in comparison with case 1. Also, the average sound pressure level at the channel outlet (microphone 3) reduces about 21 dB compared to its inlet area (microphone 1).

In case 3, the average sound pressure level rises by moving the flow along the air supply system axis and then decreases until its value at the channel entrance. This is due to the fact the same as in case 2, that with the progression of the flow inside the air supply system, a sudden change in the cross-section of the channel air supply system occurs, the boundary layer and the permeation vortices in the fluid flow are not allowed to grow. As a result, the average sound pressure level at the channel inlet (microphone 1) is less about 13 dB when compared to case 2. The average velocity of the fluid decreases when it reaches the plenum chamber.

On the other hand, due to the asymmetrical inlet and outlet of the plenum chamber, asymmetric corners are created in the chamber and generate high-strength vortices in the fluid flow. However, the average sound pressure level in the middle of the channel (microphone 2) is 28 dB more or less than in case 1. As the flow reaches the end of the channel, in addition to the sharp corner effect of the plenum chamber outlet on the flow, the boundary layer grows continually from inside the plenum chamber to the channel outlet. As a result, the average sound pressure level at the channel outlet (microphone 3) experiences a drop by roughly 31 dB more than case 1. Additionally, the average sound pressure level at the channel outlet (microphone 3) decreases about 4 dB more than its inlet area (microphone 1).

In case 4, as in case 3, the average sound pressure level rises by moving the flow along the air supply system axis and then decreases more than its value at the channel entrance. This is because of the fact that with the progression of the flow inside the air supply system, where the sudden change in the cross-section exists, the boundary layer and the permeation vortices in the fluid flow are not allowed to grow. However, the average sound pressure level at the channel inlet (microphone 1) is 5 dB more than in case 3. As flow into the plenum chamber, the average flow velocity reduces, but the boundary layer continues to grow steadily. Based on the asymmetrical inlet and outlet of the plenum chamber, geometrically, asymmetric corners are created in the chamber and it causes high-strength vortices in the fluid flow. This increases the average sound pressure level in the middle of the channel (microphone 2) to a value of 37 dB more than case 1. When the flow reaches the end of the channel, in addition to the sharp corner effect of the plenum chamber outlet on the flow, the boundary layer that has grown continually from the channel entrance will interfere with the wall of the plenum chamber at the outlet. This interference increases the turbulence of the flow and generates high-strength vortices in the fluid flow. Therefore, the average sound pressure level at the channel outlet (microphone 3) reduces approximately 2 dB less than case 1. Additionally, the average sound pressure level at the channel outlet (microphone 3) sees a rise by nearly 21 dB than its inlet area (microphone 1).

In case 5, the average sound pressure level rises by moving the flow along the air supply system axis and then decreases to its value at the channel entrance. This is because with the progression of the flow inside the air supply system, where cross-section changes suddenly, the boundary layer and the permeation vortices of fluid are not allowed to grow. As a result, the average sound pressure level at the channel inlet (microphone 1) is about 16 dB less than in case 4. Alongside the flow within the plenum chamber, the average flow velocity decreases, but the boundary layer on the one side continues to grow steadily. Because of the asymmetrical inlet and outlet of the plenum chamber, geometrically, asymmetric corners are created in the chamber and it causes high-strength vortices. This increases the average sound pressure level in the middle of the channel (microphone 2) to 13 dB more than case 1. As the flow reaches the end of the channel, in addition to the sharp corner effect of the plenum chamber outlet on the flow, the boundary layer that has grown continually from the channel entrance will interfere alongside the wall of the plenum chamber at the outlet. This interference increases the turbulence of the flow and generates high-strength vortices in the fluid flow. As a result, the average sound pressure level at the channel outlet (microphone 3) reduces by the amount of 39 dB less than in case 1.

Case 6, the same as case 2, the average sound pressure level rises as flow moves along the axis of the air supply system, and then decreases less than its value at the channel entrance. This is due to the fact that like in case 5, with the progression of the flow inside the air supply system, where there is an abrupt change in the cross-section, the boundary layer and the permeation vortices in the fluid flow are prevented from growing. On the other hand, the location of the inlet and outlet with respect to the plenum chamber will actually create a barrier to the flow and effectively reduce the effective cross-sectional area of the inlet air channel. As a result, changes in velocity and pressure fluctuations are large, so that the average sound pressure level at the channel inlet (microphone 1) is approximately 38 dB more than in case 5. As the flow into the plenum chamber, the average flow velocity reduces, but the boundary layer on the one side continues to grow steadily. In addition to it, the asymmetrical inlet and outlet of the plenum chamber, geometrically, asymmetric corners are created in the chamber and make more high-strength vortices. However, this increases the average sound pressure level in the middle of the channel (microphone 2) to 0.76 dB more than case 1. As the flow reaches the end of the channel, in addition to the sharp corner effect of the plenum chamber outlet on the flow, the boundary layer that has grown continually from the channel entrance will interfere with the wall of the plenum chamber at the outlet. Consequently, the average sound pressure level at the channel outlet (microphone 3) decreases 35 dB more than in case 1.

4.4.2. Acoustic performance evaluation of the marine gas turbine air supply system at the dominant frequency

The effects of a flow passage were ignored, and it was assumed that only plane waves can be propagated in the air supply system. Thus, the geometric dimensions of the channel at the dominant frequency of the system have been determined. In this section, the sound waves propagated in the air supply system,

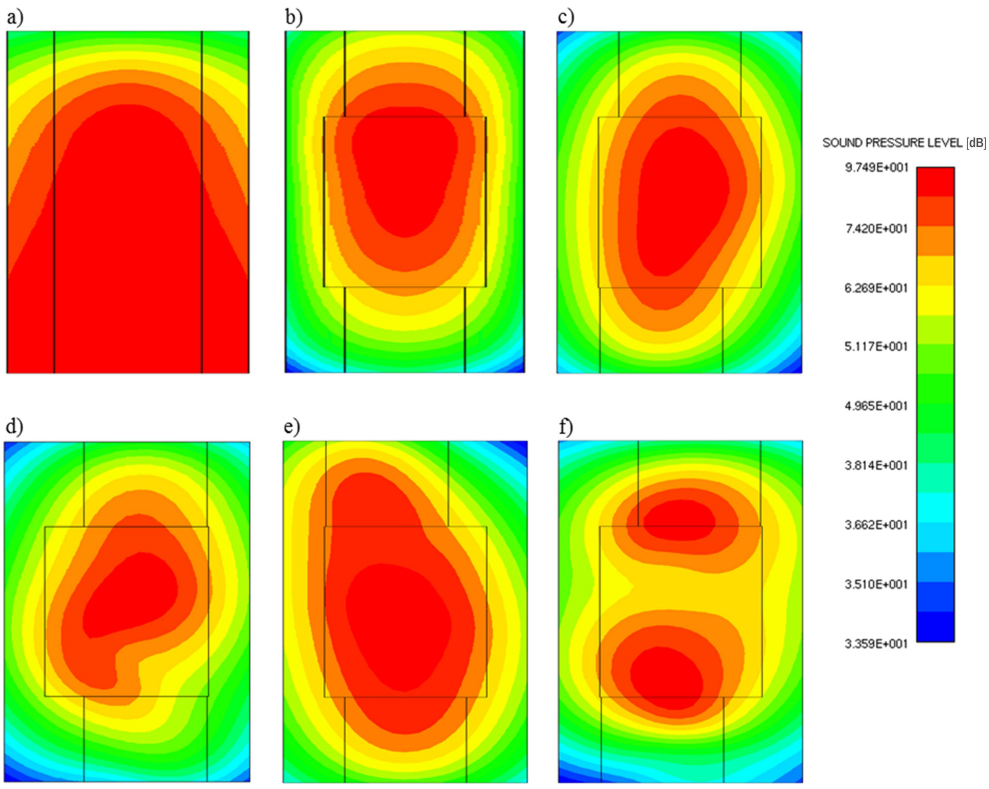

Fig. 15. The contour of sound pressure level on the receiver surface in the dominant frequency for: a) case 1, b) case 2, c) case 3, d) case 4, e) case 5, f) case 6.

taking into account the effects of the flow through it, have been studied. The contour of the sound pressure level on the receiver surface at a frequency of 23 Hz in different cases of the inlet and outlet element relative to the position of the plenum chamber is shown in Fig. 15.

In all cases, by taking into account the effects of the flow passage, there is a deviation from the propagation of plane waves in the marine gas turbine air supply system. This is due to the effects of flow through the air supply system, as well as the effect of quadruple sources of noise generation, which results in the creation of higher-level modes in the air supply system. So, with regard to the effects of flow through the air supply system, sound waves will not be propagated in the form of plane waves in the system.

5. Conclusions

This present work was conducted to provide a method to evaluate the acoustic performance of the marine gas turbine air supply system with the purpose of finding the proper state of the acoustic and aerodynamic performance of the system. The following results are summarized:

- By increasing the fraction of cross-section of the plenum chamber to the inlet or outlet of the channel, the aerodynamic performance of the air supply system reduces (rising in the pressure drop). Its acoustic performance first increases and then decreases, as well.
- By examining and comparing both cases of with and without a change in cross-section, the acoustic performance in different cases, in which proportional to inlet and outlet changes, it was found that the level of sound pressure level around the air supply channel system as well as the high-pressure sound area, could move along the air supply channel system. The minimum and maximum amount of sound pressure level at the inlet, plenum chamber and outlet channel of the marine gas turbine air supply system occurred in cases 5, 1, 2, and 6, 2, 1, respectively.
- In all cases of the marine gas turbine air supply system, based on the effects of flow, there was a deviation from the propagation of plane waves. This is due to the effects of flow through the air supply system, as well as the effect of quadruple sources of noise generation. These results in the creation of higher-level modes in the air supply system. As a consequence, by regarding the effects of flow through the air supply system, sound waves were not propagated in the form of plane waves in the system.
- In order to determine the proper configuration of the marine gas turbine air supply system, it should

be considered that the battleship engine room is in its lower floors; therefore, a large part of the bottom of the marine gas turbine air supply system is always under the buoyancy storage battleship (below sea level). On the other hand, the purpose of this design is to produce and propagate the lowest noise generated by the flow of air, which prevents the battleship to be detected via submarine sonar waves of the enemy. Therefore, the air supply system configuration in cases 5, 2, 6, and 3 are the best choice, where the lowest amount of sound pressure level occurs around the end of the system. So, this case is recommended for this application.

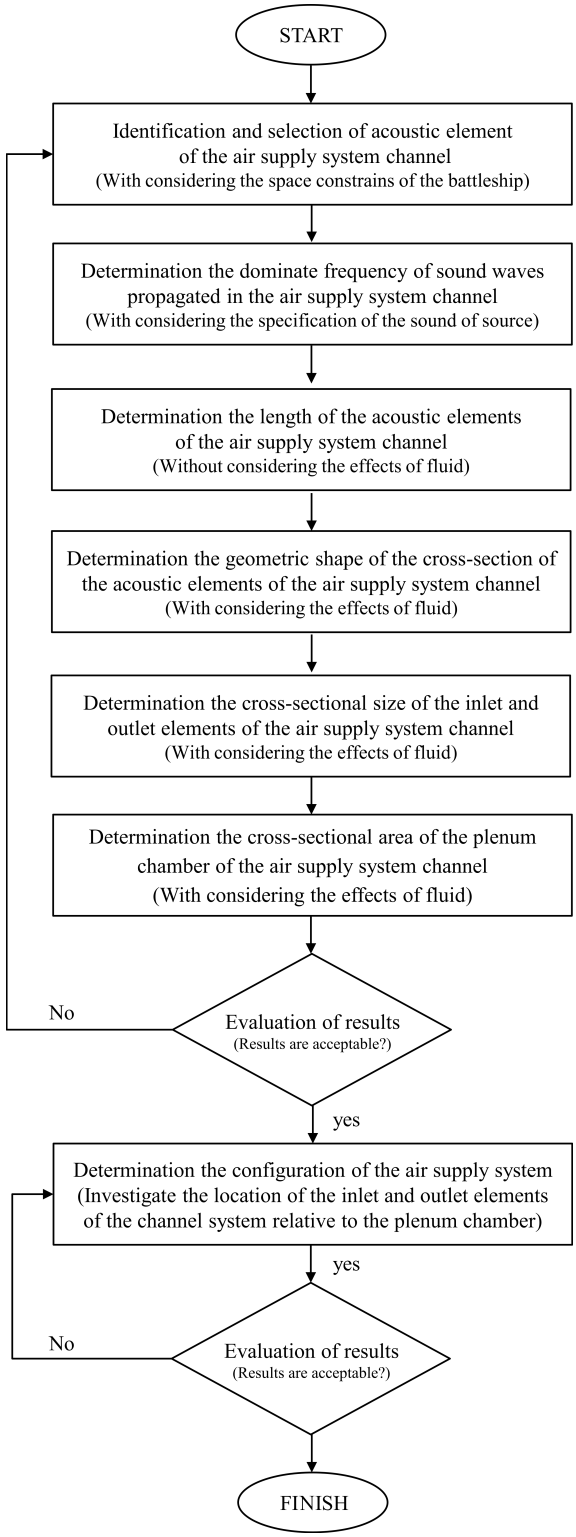

Fig. 16. Marine gas turbine air supply system design algorithms.

- According to the articles presented in different sections, an algorithm for designing a marine gas turbine air supply system that expresses the design process of the system and other similar systems is extracted (Fig. 16).

References

1. Alkan B., Atayilmaz S.O. (2018), *A hybrid numerical/experimental study of the aerodynamic noise prediction*, Journal of Thermal Engineering, **4**, 4, 2201–2210, doi: 10.18186/journal-of-thermal-engineering.434037.
2. Bies D.A., Hansen C., Howard C. (2017), *Engineering noise control*, CRC Press.
3. Bilawchuk S., Fyfe K.R. (2003), *Comparison and implementation of the various numerical methods used for calculating transmission loss in silencer systems*, Applied Acoustics, **64**, 9, 903–916, doi: 10.1016/S0003-682X(03)00046-X.
4. Cao Y., Ke H., Lin Y., Zeng M., Wang Q. (2017), *Investigation on the flow noise propagation mechanism in simple expansion pipelines based on synergy principle of flow and sound fields*, Energy Procedia, **142**, 3870–3875, doi: 10.1016/j.egypro.2017.12.290.
5. Carlton J.S. (2012), *Marine propellers and propulsion*, 3 ed., J.S. Carlton [Ed.], Oxford: Elsevier Science.
6. Chiu M.-C., Chang Y.-C. (2014), *An assessment of high-order-mode analysis and shape optimization of expansion chamber mufflers*, Archives of Acoustics, **39**, 4, 489–499, doi: 10.2478/aoa-2014-0053.
7. Chu C.I., Hua H.T., Liao I.C. (2001), *Effects of three-dimensional modes on acoustic performance of reversal flow mufflers with rectangular cross-section*, Computers & Structures, **79**, 8, 883–890, doi: 10.1016/S0045-7949(00)00184-X.
8. Dawkins S. (2011), *A guide to aeroacoustics: an overview, lighthill's equation, related model equations*, Etc: BiblioBazaar.
9. Dube R., Parmar A., Thakor R., Vasadia S., Mistri C., Sompura M. (2018), *Numerical analysis of flow induced vibrations of tubes banks in cross flow using porous media*, International Research Journal of Engineering and Technology, **5**, 5, 1496–1501, https://www.irjet.net/archives/V5/i5/IRJET-V5I5283.pdf.
10. Guasch O., Pont A., Baiges J., Codina R. (2016), *Concurrent finite element simulation of quadrupolar*

and dipolar flow noise in low Mach number aeroacoustics, Computers & Fluids, **133**, 129–139, doi: 10.1016/j.compfluid.2016.04.030.

11. Guasch O., Pont A., Baiges J., Codina R. (2017), *Simultaneous finite element computation of direct and diffracted flow noise in domains with static and moving walls*, Paper presented at the International Conference on Flow Induced Noise and Vibration Issues and Aspects.
12. Hillenbrand J., Becker S., Sailer T., Wetzel M., Hausner O. (2016), *Numerical simulation of turbulence induced flow noise in automotive exhaust systems using scale-resolving turbulence models*, Springer.
13. Howe M.S. (2003), *Theory of vortex sound*, Cambridge University Press.
14. Ji Z.L. (2005), Acoustic attenuation performance analysis of multi-chamber reactive silencers, *Journal of sound and vibration*, **283**, 1–2, 459–466, doi: 10.1016/j.jsv.2004.05.013.
15. Kårekull O., Efraimsson G., Åbom M. (2014), *Prediction model of flow duct constriction noise*, Applied Acoustics, **82**, 45–52, doi: 10.1016/j.apacoust.2014.03.001.
16. Łapka W. (2014), *Acoustic attenuation performance of a round silencer with the spiral duct at the inlet*, Archives of Acoustics, **32**, 4(S), 247–252.
17. Lighthill M.J. (1952), *On sound generated aerodynamically. I. General theory*, Proceedings of the Royal Society of London. Series A, Mathematical and Physical Sciences, **211**, 1107, 564–587, doi: 10.1098/rspa.1952.0060.
18. Liu E., Yan S., Peng S., Huang L., Jiang Y. (2016), *Noise silencing technology for manifold flow noise based on ANSYS fluent*, Journal of Natural Gas Science and Engineering, **29**, 322–328, doi: 10.1016/j.jngse.2016.01.021.
19. Maizi M., Mohamed M.H., Dizene R., Mihoubi M.C. (2018), *Noise reduction of a horizontal wind turbine using different blade shapes*, Renewable Energy, **117**, 242–256, doi: 10.1016/j.renene.2017.10.058.
20. Mak C.M., Wang X., Ai Z.T. (2014), *Prediction of flow noise from in-duct spoilers using computational fluid dynamics*, Applied Acoustics, **76**, 386–390. doi: 10.1016/j.apacoust.2013.08.021.
21. Mohammed R., Sabry A., Abd El-Gwwad K.A., Abd-El-Tawwab A.M., Nouby M. (2012), *Modelling and analysis of single expansion chamber using Response Surface Methodology*, Journal of Engineering Research and Applications (IJERA), **2**, 1, 651–658, http://www.ijera.com/papers/Vol2_issue1/DA216516-58.pdf.
22. Munjal M.L. (1997), *Plane wave analysis of side inlet/outlet chamber mufflers with mean flow*, Applied Acoustics, **52**, 2, 165–175, doi: 10.1016/S0003-682X(96)00053-9.
23. Munjal M.L. (1987), *Acoustics of ducts and mufflers with application to exhaust and ventilation system design*, New York: Wiley.
24. Nag S., Gupta A., Dhar A. (2017), *Sound attenuation in expansion chamber muffler using plane wave method and finite element analysis*, Nonlinear Studies, **24**, 1, 69–78, http://nonlinearstudies.com/index.php/nonlinear/article/view/1464.
25. Nakayama Y., Boucher R.F. (1998), *Introduction to fluid mechanics*, Oxford: Butterworth-Heinemann.
26. Norton M.P., Karczub D.G. (2003), *Fundamentals of noise and vibration analysis for engineers*, Cambridge University Press.
27. Peng Z., Fan J., Wang B. (2018), *Analysis and modelling on radiated noise of a typical fishing boat measured in shallow water inspired by AQUO Project's Model*, Archives of Acoustics, **43**, 2, 263–273, doi: 10.24425/122374.
28. Sagaut P. (2001), *Large Eddy Simulation for incompressible flows. An introduction*, Measurement Science and Technology, **12**, 10, 1745, doi: 10.1088/0957-0233/12/10/707.
29. Tsuji T., Tsuchiya T., Kagawa Y. (2002), *Finite element and boundary element modelling for the acoustic wave transmission in mean flow medium*, Journal of Sound and Vibration, **255**, 5, 849–866, doi: 10.1006/jsvi.2001.4189.
30. Vizzini S., Knutsson M., Dybeck M., Ĺbom M. (2018), *Flow Noise Generation in a Pipe Bend*, SAE Technical Paper 2018-01-1525, doi: 10.4271/2018-01-1525.
31. Wang M., Freund J.B., Lele S.K. (2006), *Computational prediction of flow-generated sound*, Annual Review of Fluid Mechanics, **38**, 483–512, doi: 10.1146/annurev.fluid.38.050304.092036.
32. Warczek J., Burdzik R., Konieczny Ł., Siwiec G. (2017), *Frequency analysis of noise generated by pneumatic wheels*, Archives of Acoustics, **42**, 3, 459–467, doi: 10.1515/aoa-2017-0048.
33. Wilcox D.C. (1998), *Turbulence modeling for CFD* (3 ed.), DCW Industries.
34. Wu C.J., Wang X.J., Tang H.B. (2007), *Transmission loss prediction on SIDO and DISO expansion-chamber mufflers with rectangular section by using the collocation approach*, International Journal of Mechanical Sciences, **49**, 7, 872–877, doi: 10.1016/j.ijmecsci.2006.11.007.
35. Wu C.J., Wang X.J., Tang H.B. (2008), *Transmission loss prediction on a single-inlet/double-outlet cylindrical expansion-chamber muffler by using the modal meshing approach*, Applied Acoustics, **69**, 2, 173–178, doi: 10.1016/j.apacoust.2006.06.011.
36. Zhang Z., Li J., Mak C.M. (2009), *Simulation analysis of acoustic attenuation performance for different shape of an expansion chamber silencer*, Paper presented at the 2009 Second International Conference on Information and Computing Science.